

# DSMC Modeling of Internal Energy Excitation and Dissociation of Molecular Nitrogen in Hypersonic Reentry Flows

Zheng Li, Ilyoung Sohn, Deborah A. Levin

*Department of Aerospace Engineering, The Pennsylvania State University, University Park, PA 16802*

**Abstract.** The current work implemented in DSMC vibrational excited levels of  $N_2$  and transitions between the levels as well as the dissociation of nitrogen molecules from different levels. Results show that due to insufficient collisions, the flow around a sphere at 70/75 km altitudes has a high degree of nonequilibrium in the vibrational mode where the ground level is separated from the higher levels. The continuum-level calculation results are different from the work of Candler and the nonequilibrium profile predicted by the discrete-level calculation is also different.

**Keywords:** DSMC, Kinetic Theory

**PACS:** 47.55.Ca

## INTRODUCTION

For high-speed reentry vehicles, such as Stardust [1], various physico-chemical processes are important in the design of heat shields. Due to the rapid increase of high translational energy of the gas as it passes through an intense shock, these strongly-coupled processes include excitation of the internal energy modes, molecular dissociation, ionization and radiation of the atoms and molecules. Particle simulation methods, such as direct simulation Monte Carlo (DSMC) [2] method, are required to accurately simulate high-speed reentry flow at high altitudes since continuum breakdown occurs due to the strong shock condition.

Most previous DSMC calculations assume the gas to be in the electronic ground state, and energies are assigned continuously to translational, rotational, and vibrational modes. Our previous work [3] addressed the concern of the excitation of the atoms by implementing excited energy levels of atomic N and O with the corresponding electron impact excitation/de-excitation and ionization processes in DSMC. The results show that when excitation-state models are included, there is a small but observable increase in the ion number densities and electron temperatures for the Stardust 68.9 km re-entry flow. Adding in the excited levels of atoms increases the degree of ionization by providing additional intermediate steps towards ionization.

The work that will be discussed in this paper builds on the previous work by replacing the continuous internal energy model with higher fidelity collisional radiative (CR) [4] models. In general the three types of CR models, in increasing order of complexity and computational time, are: electronic, vibrational and rovibrational CR models. In electronic CR models, transitions between the electronic states are considered and the rotational and vibrational temperatures,  $T_r$  and  $T_v$ , of the molecules are obtained by internal energy exchange models through collisions. In vibrational CR models, transitions between the vibrational states of the molecules are also considered and only a rotational temperature  $T_r$  is computed. Finally, in ro-vibrational CR models, no temperature is used to describe the molecular internal energy. Vibrational CR models will be implemented in DSMC and transitions between the vibrational excited states of the nitrogen molecules as well as the dissociation of nitrogen molecules from different vibrational excited states will be considered.

## VIBRATIONAL COLLISION RADIATIVE MODEL

**Vibrational energy** of  $N_2$  molecules can be specified on the base of simple harmonic oscillator (SHO) model. In this case, the vibrational energy level of  $V$  is given by

$$E_v(V) = k\theta_v(V + 0.5), V = 0, 1, 2, \dots, V_{max}, \quad (1)$$

where  $k$  is the Boltzmann constant and  $\theta_v$  is the characteristic temperature of vibration. The maximum level  $V_{max} = [E_d/k\theta_v]$  where  $E_d$  is the dissociation energy and  $[\dots]$  denotes the truncation.

The **equilibrium distribution function** for SHO is

$$f_v(V, T) = \frac{g_v e^{-\frac{E_v(V)}{kT}}}{Q(T)}, \quad (2)$$

where degeneracy  $g_v \equiv 1$  and  $Q(T)$  is the partition function

$$Q(T) = \sum_{V=0}^{V_{max}} \exp\left(-\frac{\theta_v}{T}(V+0.5)\right) = e^{-\frac{\theta_v}{2T}} \frac{1 - \exp\left(-\frac{\theta_v}{T}(V_{max}+1)\right)}{1 - \exp\left(-\frac{\theta_v}{T}\right)} \approx \frac{e^{-\frac{\theta_v}{2T}}}{1 - e^{-\frac{\theta_v}{T}}}, \quad (3)$$

So,

$$f_v(V, T) = \left(1 - e^{-\frac{\theta_v}{T}}\right) e^{-\frac{V\theta_v}{T}}, \quad (4)$$

At **particle initialization**, particle reflection on the surface, and inflow particle sampling, Boltzmann distribution at temperature  $T$  is used for specifying vibrational levels of new molecules. The algorithm works as follows:

1. Select a random number  $0 \leq R \leq 1$ ;
2. Find  $V$  so that  $\sum_{l=0}^V f_v(l, T) \geq R$ ;
3. Set  $V$  as the vibrational level of the new molecule.

The **VT energy transfer** occurs when  $N_2(V) + N_2 \rightleftharpoons N_2(V') + N_2$ . The sum  $E_c$  of relative translational energy  $E_{tr}$  and vibrational energy  $E_v$  of selected molecule is redistributed according to the local equilibrium distributions. The algorithm works as follows:

1. Select a random number  $0 \leq R_1 \leq 1$ ;
2. Let  $l = R_1 * (V_{max} + 1)$ ;
3. Select another random number  $0 \leq R_2 \leq 1$ ;
4. If  $R_2 < F(l)/F_{max}$ , set  $V' = l$ ,  $E'_{tr} = E_c - E_v(l)$ , and exit;
5. Otherwise, go to step 2.

Here  $F(V) \propto (E_c - E_v(V))^{1-\alpha}$  and  $F_{max} \equiv E_c^{1-\alpha}$ .

The **VV energy transfer** occurs when  $N_2(V) + N_2(W) \rightleftharpoons N_2(V') + N_2(W')$ . The sum  $E_c$  of relative translational energy  $E_{tr}$  and vibrational energies  $E_v(V)$  and  $E_v(W)$  is redistributed according to the local equilibrium distributions. The algorithm works as follows:

1. Select two random numbers  $0 \leq R_1, R_2 \leq 1$ ;
2. Let  $l = R_1 * (V_{max} + 1)$  and  $m = R_2 * (V_{max} + 1)$ ;
3. Select another random number  $0 \leq R_3 \leq 1$ ;
4. If  $R_3 < F(l, m)/F_{max}$ , set  $V' = l$ ,  $W' = m$ ,  $E'_{tr} = E_c - E_v(l) - E_v(m)$ , and exit;
5. Otherwise, go to step 2.

Here  $F(V, W) \propto (E_c - E_v(V) - E_v(W))^{1-\alpha}$  and  $F_{max} \equiv E_c^{1-\alpha}$ .

The **dissociation** occurs when  $N_2(V) + N_2 \rightarrow N + N + N_2$ . The total collision energy model is used for the chemical reaction. In the TCE model, the dissociation occurs when the collision energy  $E_c = E_{tr} + E_v(V)$  is greater than the dissociation energy  $E_d$ . The reaction probability has a special form,  $P(E_c)$ , that allows one to match experimental reaction rates  $K_f(T)$  in modified Arrhenius form. When the dissociation occurs, firstly, the collision energy  $E_c$  is reduced to  $E'_c = E_c - E_d$ . Then an inelastic collision between  $N_2(V)$  and  $N_2$  is performed based on momentum and energy conservation laws; and the post-collisional velocities of  $N_2(V)$  and  $N_2$  are  $\vec{v}_{N_2(V)}^*$  and  $\vec{v}_{N_2}^*$ . The last stage of the dissociation process is that the  $N_2(V)$  molecule decomposes into two N atoms,  $N_A$  and  $N_B$ . Their velocities are determined as

$$m_{N_A} \vec{v}_{N_A} + m_{N_B} \vec{v}_{N_B} = m_{N_2(V)} \vec{v}_{N_2(V)}^* \quad (5)$$

$$\vec{v}_{N_A} - \vec{v}_{N_B} = \left( \frac{4E_{int}^{N_2(V)}}{m_N} \right)^{1/2} \vec{e} \quad (6)$$

where  $\vec{e}$  is a random unit vector. Thus, the entire internal energy of the molecule  $N_2(V)$  is transferred into the energy of the relative motion of the atoms.

## NUMERICAL FLOW MODELING TECHNIQUE IN DSMC

The above models were applied to the DSMC simulations of a 5 km/s flow around a 10 cm sphere with a wall temperature of 500 K at the altitude of 75 km or 70 km. In the simulations, two species (N and  $N_2$ ) and the formentioned dissociation reaction were considered. The freestream conditions of pure molecular nitrogen modeled for temperature, number density, and  $K_{n,\infty}(L = 0.01 \text{ m})$  were 200.2 K,  $9.33 \times 10^{20} \text{ molec/m}^3$ , and 0.12 at 75 km, and, 219.7 K,  $1.88 \times 10^{21} \text{ molec/m}^3$ , and 0.65 at 70 km, respectively. The DSMC method was implemented in the Statistical Modeling In Low-density Environment (SMILE)[5] computational tool. Majorant frequency scheme was used for pair selections, variable hard sphere model was used for collisions and Borgnakke-Larsen model was used for internal energy exchange. In the simulations, 180,000 simulated particles, 32,000 collisional cells and 32,000 macro parameter cells are used. The time step was  $2 \times 10^{-7} \text{ s}$  and the sampling was done with 9,000 steps before 1,000 pre-sampling steps.

## RESULTS AND DISCUSSIONS

Figure 1 shows the number density and translational temperature contours for flow around the sphere at 75 km without dissociation. In this case, the continuum vibrational level model is applied. At 70 km, the flow is transitional and the shock is thick compared to a continuum case. The maximum total density of  $5 \times 10^{22}$  is observed at stagnation point of the body and the maximum translational temperature is 14,000 K inside the shock.

Figure 2 shows the comparisons of the number density and translational/vibrational temperatures along the stagnation line with continuum vibrational levels and discrete levels. The case has no dissociation. It can be that both density and temperatures are unchanged whether discrete levels are applied or not. The replacement of continuum levels  $E_v$  with discrete levels  $E_v(V)$  digitalized the levels. In this work, the same universal relaxation mechanism/rate is applied, *i.e.*, after the vibrational energy is added to the total collisional energy, same rate based on the collisional energy is applied. Therefore, the flow field is unchanged. Similarly in Fig. 3, when dissociation reactions is enabled, the results are unchanged since the same universal reaction rate is applied. In addition, since the flow velocity is not high, the degree of dissociation or the atomic nitrogen mole fraction is low.

When the vibrational populations (number density for different vibrational levels) are examined, it can be seen in Fig. 4, at 75 km, in the freestream, where the temperature is low (200 K), only the ground state ( $V = 0$ ) is present. As the flow temperature increases along the stagnation line, newly created excited  $N_2$  molecules follow a Boltzmann distribution (equally spaced on the log scale). The separation of the ground state with excited states are due to fact that a large portion of  $N_2$  ground state molecules do not experience collisions and stay at the level. At this altitude, there are not enough collisions so that the vibrational levels of the  $N_2$  molecules follow a Boltzmann distribution. At 70 km, where the number density doubles, the middle part of the figure shows that the difference between ground and excited levels are reduced due to higher collision rate. However, there are still not enough collisions. In the right part of the figure, an artificial case with the density at 70 km and a temperature of 5,000 K was investigated. In this case, since the temperature is high, the particles experience a large number of collisions, the  $N_2$  follows a Boltzmann distribution which indicates the validity of our algorithm. The large difference near the wall is due to the low wall temperature.

When compared our results with the work of Candler *et al.* [6] where a continuum method with implementation of discrete levels is applied, Fig. 5 shows the translational/vibrational temperatures along the stagnation line with continuum vibrational levels at 75 km. It can be seen that our simulation predicts similar maximum translational and vibrational temperatures as theirs. However, the shock stand distance is doubled. The difference could due to the continuum/particle methodology as well as the different parameters used in both works. The discrepancy will be investigated in detail in the future. In the figure, the numbers 1 ... 6 and letters A ... B represent different locations on the stagnation line with 1 and A in the free stream and 6 and D closest to the wall.

Finally, the comparison of the vibrational populations from both works at 75 km without dissociation is shown in Fig. 6. In the work of Candler *et al.*, the degree of non-equilibrium in vibrational mode can be seen since the lines are not straight. However, in our work, it is obvious that the ground state is separated from the excited levels and the excited levels are following Boltzmann distribution. The separation is not observed in their work. Further investigation will be made to resolve this issues.

## SUMMARY

The current work implemented in DSMC vibrationally excited levels of  $N_2$  and transitions between the levels as well as the dissociation of nitrogen molecules from different levels. Results show that due to insufficient collisions, the flow around a sphere at 70/75 km altitudes has a high degree of nonequilibrium in the vibrational mode where the ground level is separated from the higher levels. The continuum-level calculation results are different from the work of Candler and the nonequilibrium profile predicted by the discrete-level calculation is also different. Since the current model uses a universal relaxation/dissociation rate, the discrete-level and continuum-level simulation results are close. Further investigation will be made to introduce individual relaxation/dissociation rate to utilize the advantage of the discrete model. The difference with Candler's work will be studied in detail.

## ACKNOWLEDGMENTS

The research performed at the Pennsylvania State University was supported by the NASA through the Grant No. NNX07AC47A. We would like to acknowledge Prof. M. Ivanov of the Institute of Theoretical and Applied Mechanics, Russia for the use of the original SMILE code.

## REFERENCES

1. D. Olynick, Y. Chen, and M. Tauber, *Journal of Spacecraft and Rockets* **36**, 442–462 (1999), ISSN 0022-4650.
2. G. A. Bird, *Molecular Gas Dynamics and the Direct Simulation of Gas Flows*, Clarendon Press, 1994.
3. T. Ozawa, I. Sohn, Z. Li, D. A. Levin, and M. M. Modest, Modeling of electronic excitation and radiation for hypersonic reentry flows in dsmc, AIAA paper 2010-0987 (2010).
4. T. Margin, M. Panesi, A. Bourdon, R. Jaffe, and D. Schwenke, Internal energy excitation and dissociation of molecular nitrogen in a compressing flow, AIAA paper 2009-3887 (2010).
5. M. S. Ivanov, A. V. Kashkovsky, S. F. Gimelshein, G. N. Markelov, A. A. Alexeenko, Y. A. Bondar, G. A. Zhukova, S. B. Nikiforov, and P. V. Vashenkov, "SMILE System for 2D/3D DSMC computations," in *Proceedings of the 25th International Symposium on Rarefied Gas Dynamics*, edited by M. S. Ivanov, and A. K. Rebrov, Publishing House of the Siberian Branch of the Russian Academy of Sciences, Novosibirsk, 2007, pp. 539–544.
6. G. V. Candler, J. Olejniczak, and B. Harrold, *Physics of Fluids* **9**, 2108–2117 (1997).

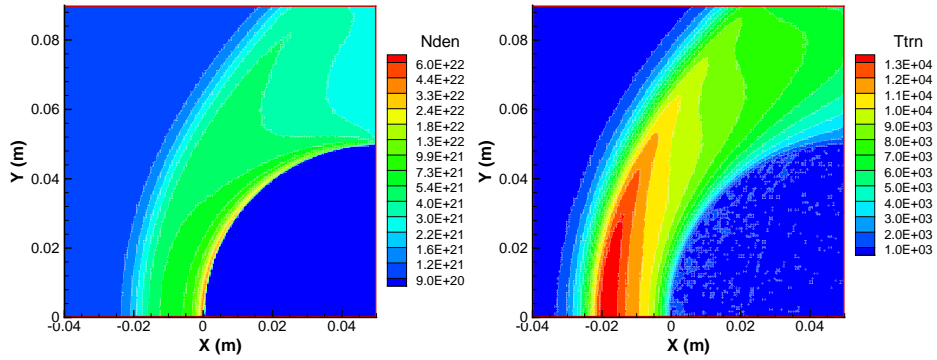


**FIGURE 1.** Number density (left) and translational temperature (right) contours for flow around a 10 cm sphere at 75 km without dissociation. Continuum vibrational level model is applied.

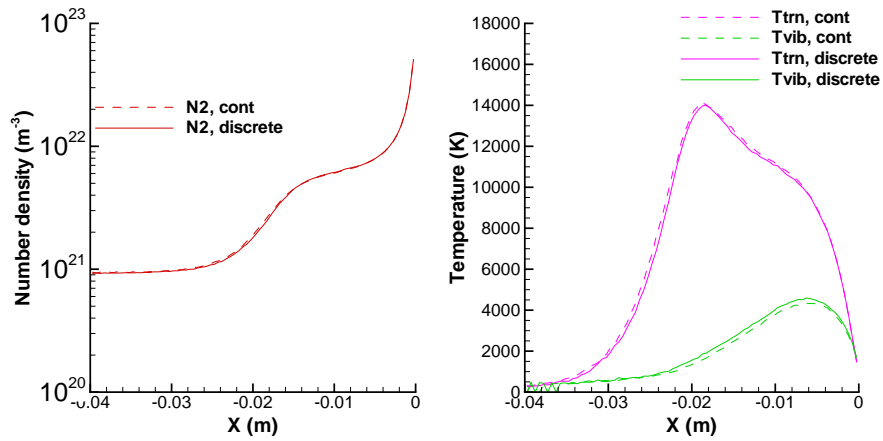


**FIGURE 2.** Number density (left) and translational/vibrational temperatures (right) along the stagnation line with continuum vibrational levels and discrete levels. The case has no dissociation and the wall is at  $X = 0$ .

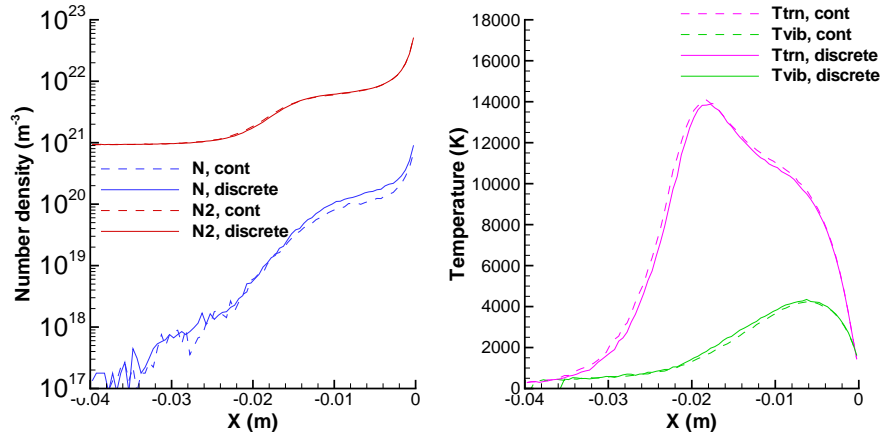


**FIGURE 3.** Number density (left) and translational/vibrational temperatures (right) along the stagnation line with continuum vibrational levels and discrete levels. The case has dissociation.

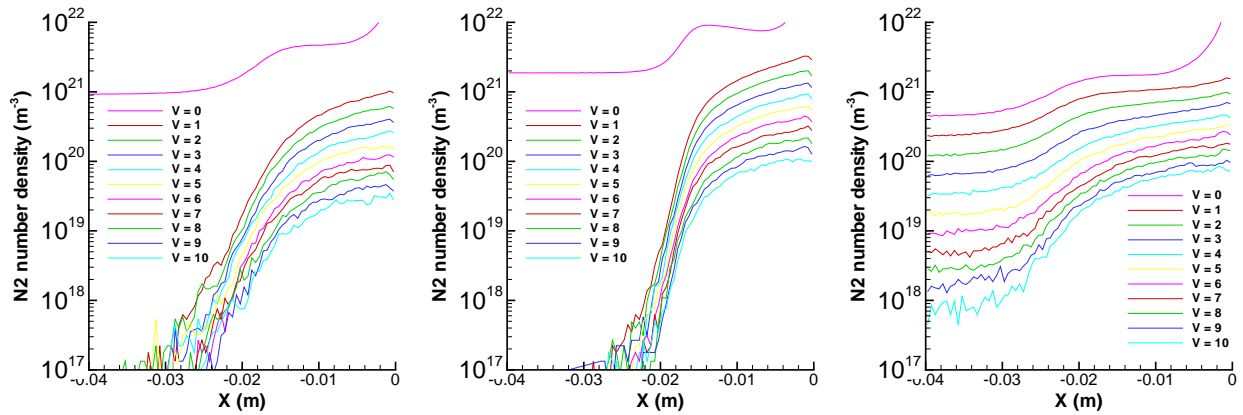


**FIGURE 4.** Vibrational populations along the stagnation line without dissociation at 70 km (Left), 75 km (middle) and 70 km/5000 K (right).

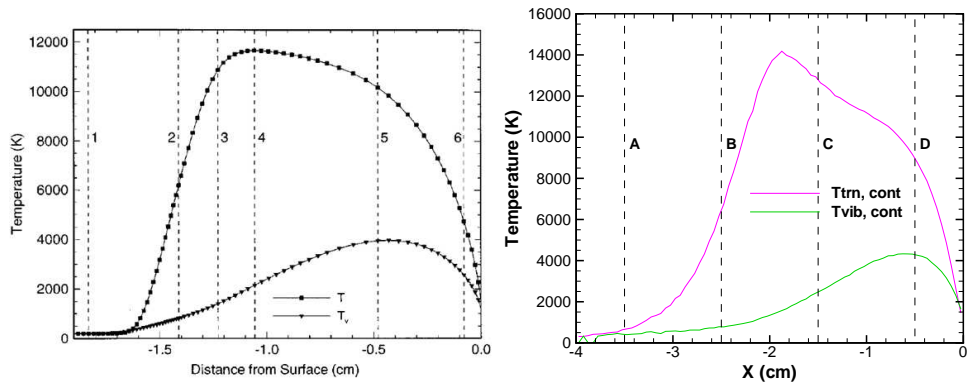


**FIGURE 5.** Comparison of translational/vibrational temperature from the work of Candler *et al.* (left) and DSMC along the stagnation line at 75 km with discrete vibrational levels and without dissociation.

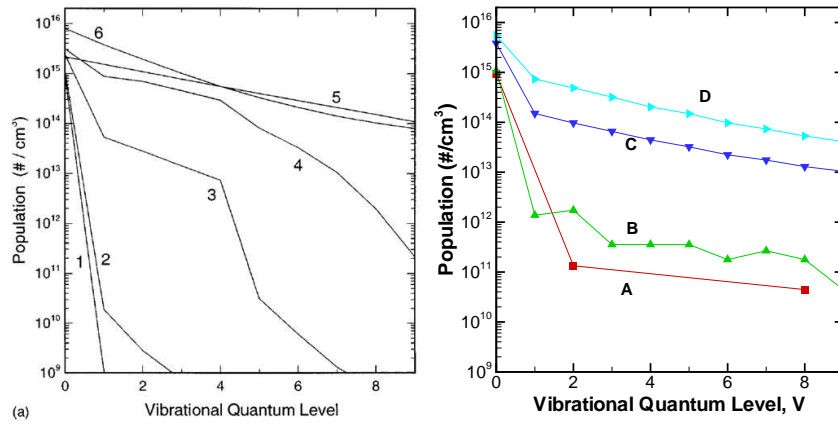


**FIGURE 6.** Comparison of vibrational populations from the work of Candler *et al.* (left) and DSMC along the stagnation line at 75 km with discrete vibrational levels and without dissociation.